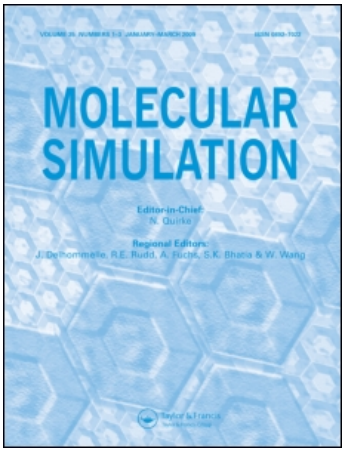

Molecular Simulation
Publication details, including instructions for authors and subscription information:
http://www.informaworld.com/smpp/title~content=t713644482

Rational, Hierarchical Parameterization of Complex Zeolite-guest Molecular Models

M. A. Snyder[a]; D. G. Vlachos[a]
[a] Department of Chemical Engineering and Center for Catalytic Science and Technology (CCST), University of Delaware, Newark, DE, USA

To cite this Article Snyder, M. A. and Vlachos, D. G.(2004) 'Rational, Hierarchical Parameterization of Complex Zeolite-guest Molecular Models', Molecular Simulation, 30: 9, 561 — 577
To link to this Article: DOI: 10.1080/08927020410001717245
URL: http://dx.doi.org/10.1080/08927020410001717245

Molecular Simulation, VOL. 30 (9), 10 August 2004, pp. 561–577

Taylor & Francis
Taylor & Francis Group

Rational, Hierarchical Parameterization of Complex Zeolite-guest Molecular Models

M.A. SNYDER and D.G. VLACHOS*

Department of Chemical Engineering and Center for Catalytic Science and Technology (CCST), University of Delaware, Newark, DE 19716, USA

(Received January 2004; In final form March 2004)

A hierarchical approach is presented for rationally parameterizing complex molecular models of guest species in microporous materials. The large number of microscopic processes (e.g. adsorption, desorption, site-to-site migration), and intrinsic complexity of potential energy surfaces characterizing these systems, demands simultaneous optimization to multiple sets of experimental data to ensure model predictive capabilities. The first step of the approach capitalizes on the computational efficiency of mean field models to initially identify sensitive parameters and narrow the window of parameter space. Surface response techniques are subsequently employed in this window for rational optimization of the computationally intensive molecular models. The hierarchical approach is developed in light of both enthalpic and entropic constraints to ensure consistency of multiple microscopic processes. We illustrate this approach using a lattice kinetic Monte-Carlo description of benzene in NaX zeolite. Through application of simulated annealing techniques, the hierarchical framework is capable of optimizing the model parameters simultaneously to disparate sets of experimental data (e.g. adsorption isotherms and PFG-NMR self-diffusivity). Finally, application to other atomistic models is also discussed.

Keywords: Zeolites; Molecular modeling; Parameterization; Adsorption; Desorption; Molecule migration

INTRODUCTION

The field of zeolite science spans a wide range of both catalytic and non-catalytic applications, such as hydrocarbon cracking, shape-selective catalysis, pressure swing adsorption and zeolite membranes for high-resolution gas separation. Molecular modeling has emerged as a powerful tool, providing deep fundamental insight into equilibrium and non-equilibrium dynamics of molecules within these complex microporous materials. Harnessing this fundamental insight provides unprecedented opportunities to optimize existing processes, rationally direct experimental studies, speed the development of emerging technologies (e.g. coupled reaction and separation technologies), and ultimately push the frontiers of discovery towards currently unrealized materials, processes and applications.

An array of molecular modeling approaches has been employed to study these systems over a range of length and time scales. Among the most fundamental techniques is that of molecular dynamics (MD) simulations. This approach provides exact solutions to a given model, but is limited to time scales on the order of nanoseconds and length scales of nanometers [1–4]. Atomistic grand canonical Monte-Carlo (GCMC) simulations [5,6] have also been explored, where advances in configurationally biased algorithms [5,7,8] have allowed for investigation of complex molecular systems. Coarse-graining, leading to improvement in computational efficiency, is often achieved through lattice dynamic Monte-Carlo (DMC) or kinetic Monte-Carlo (KMC) simulations [9–17] employed for systems where the binding energy is relatively high compared to the thermal energy and, thus, transitions from one site to another are "rare" events compared to the vibrational time scales.

Most technologies of microporous materials involve many simultaneous microscopic mechanisms (e.g. adsorption, desorption, migration, reaction, etc.) of molecular species. Current molecular modeling, however, often focuses on subsets of these

*Corresponding author. E-mail: vlachos@che.udel.edu

ISSN 0892-7022 print/ISSN 1029-0435 online © 2004 Taylor & Francis Ltd
DOI: 10.1080/08927020410001717245

mechanisms. In particular, modeling of adsorption isotherms via GCMC is typically performed independently of studies on equilibrium diffusion (i.e. self-diffusivity). Ultimately, there is a need for self-consistent molecular simulations describing multiple microscopic mechanisms. To this end, the development of appropriate potential energy surfaces (PES) and application of atomistic or coarse-grained molecular models for predicting both equilibrium and non-equilibrium properties demands appropriate parameterization of PES and/or transition probabilities to ensure the predictive capabilities of these models. Current state of the art for such parameterization employs a tedious, manual parameter adjustment to fit crystallographic and equilibrium data. In the case where such *ad-hoc* parameterization is even feasible, the resulting models risk being ill-parameterized and limited to local agreement with fitted data rather than being able to capture system responses over a wide range of conditions (i.e. temperature, pressure, loading). In order to overcome this problem, a rational approach for parallel parameterization against multiple types and sets of data with minimum computational cost is required.

Here we propose a rational, hierarchical methodology introduced in Ref. [18] for extraction of molecular model parameters from multiple experimental measurements. Our methodology employs mean field (MF) models for rapid exploration of parameter space that guides surface response techniques for parameterization of the computationally intensive molecular models. As a result of the large number of optimizable parameters available in multiple mechanisms of complex systems, a challenge is to ensure the self-consistency of the resulting molecular model. In this work, we explore this notion of thermodynamic consistency and illustrate the capabilities of this powerful hierarchical technique by parameterizing a lattice model describing adsorption, desorption and diffusion of benzene in NaX zeolite based upon both adsorption isotherm and PFG-NMR self-diffusivity data.

MODEL SYSTEM: BENZENE IN NaX ZEOLITE

Here we consider the system of benzene in NaX zeolite, a system modeled extensively by Auerbach and co-workers [11]. Although a single-component system, the energetics of benzene in the NaX zeolite topology make it an interesting example to illustrate the capabilities of the proposed hierarchical parameterization approach. Neutron and X-ray diffraction studies of this and other similar systems (i.e. benzene in NaY zeolite) have identified predominant binding sites [19–21]. Similar to the NaY zeolite system, benzene is found to bind strongly in a facially coordinated orientation above four Na cations within the NaX supercage structure (S_{II} sites). Benzene is also believed to bind more weakly in four doubly-shared low-symmetry sites near Na(III′) cations that lie within the 12-ring windows (W sites) joining adjacent NaX supercages. As a result, the average number of binding sites per supercage is six, yet experimental evidence suggests a saturation loading of only approximately 5.4 molecules/supercage [22].

Extensive modeling work has focused on investigating self-diffusivity of benzene within this system [11]. Based on the rare-event diffusion of benzene between distinct binding sites (i.e. W and S_{II}), Auerbach and co-workers have proposed a lattice model as a coarse-grained representation of the binding sites accessed by benzene. This lattice framework, depicted in Fig. 1, consists of supercages, tetrahedrally connected via the W sites. In addition, the four S_{II} sites are tetrahedrally arranged within the supercage.

The disparate energetics of benzene within this dual-site system results in a number of distinct microprocesses characterizing adsorption, desorption and diffusion pathways. These include benzene adsorption to and desorption from both S_{II} and W sites, and three reversible site-to-site diffusion pathways of benzene among both like sites (e.g. W⇌W and S_{II}⇌S_{II}) and dissimilar sites (e.g. W⇌S_{II}). It is helpful to cast all mechanisms as a series of elementary chemical reactions, as shown in columns 2 and 3 of Table I. Each of these microprocesses is associated with a characteristic transition probability per time, Γ. A tabulation of the number of parameters available for optimization yields 8 pre-factors (e.g. rate constants for adsorption to site i ($\Gamma^0_{\mathrm{ads},i}$), desorption pre-exponentials ($\Gamma^0_{\mathrm{des},i}$), and site-to-site ($i \rightarrow j$) migration pre-exponentials ($\Gamma^0_{\mathrm{mig},ij}$)) and 9 energetic parameters (e.g. site-specific zero-coverage heats of adsorption (ε^0_i), zero-coverage activation energies of site-to-site ($i \rightarrow j$) migration ($E^0_{\mathrm{a},ij}$), and adsorbate–adsorbate intermolecular forces (J_{ij})). Note that in experimental systems, adsorption and desorption entails only

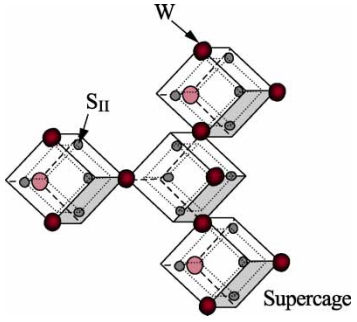

FIGURE 1 Lattice model of weak (W, window) and strong (S_{II}, intracage) binding sites for benzene in NaX zeolite. (Colour version available online.)

TABLE I Summary of microprocesses, transition probabilities, and parameter optimization results

Microprocess	*'Reaction'*	*Transition probability*	*Base parameters*	*MF optimized parameters*	*MC optimized parameters*
1. W adsorption	$B + W \rightarrow BW$	$\Gamma_{ads,W}(i) = \Gamma^0_{ads,W}(i)P(1-w_i)$	(Γ^0)*	–	–
2. W desorption	$BW \rightarrow B + W$	$\Gamma_{des,W}(i) = \Gamma^0_{des,W}(i)w_i \exp\left\{-\beta\left[\left\|\varepsilon^0_W\right| + \sum_{j\neq i} J_{WW} w_j + \sum_{k\neq i} J_{WS_{II}} s_k\right]\right\}$	1.0×10^{13} (Γ^0)	1.1×10^{14} (Γ^0)	7.8×10^{13} (Γ^0)
3. S_{II} adsorption	$B + S_{II} \rightarrow BS_{II}$	$\Gamma_{ads,S_{II}}(i) = \Gamma^0_{ads,S_{II}}(i)P(1-s_i)$	(Γ^0)*	–	–
4. S_{II} desorption	$BS_{II} \rightarrow B + S_{II}$	$\Gamma_{des,S_{II}}(i) = \Gamma^0_{des,S_{II}}(i)s_i \exp\left\{-\beta\left[\left\|\varepsilon^0_{S_{II}}\right| + \sum_{j\neq i} J_{S_{II}S_{II}} s_i + \sum_{k\neq i} J_{S_{II}W} w_k\right]\right\}$	$(\Gamma^0)^\dagger$	–	–
5. W → W migration	$BW + W \rightarrow W + BW$	$\Gamma_{mig,WW}(i) = \Gamma^0_{mig,WW}(i)w_i \sum_{j\neq i}(1-w_j)\exp\left\{-\beta\left[E^0_{a,WW} + PBJ\right]\right\}$	$2.4 \times 10^{11}(\Gamma^0)$	–	–
6. S_{II} → S_{II} migration	$BS_{II} + S_{II} \rightarrow S_{II} + BS_{II}$	$\Gamma_{mig,S_{II}S_{II}}(i) = \Gamma^0_{mig,S_{II}S_{II}}(i)s_i \sum_{j\neq i}(1-s_j)\exp\left\{-\beta\left[E^0_{a,S_{II}S_{II}} + PBJ\right]\right\}$	0.8×10^{13} (Γ^0), 14.4705 (E^0)	–	–
7. W → S_{II} migration	$BW + S_{II} \rightarrow W + BS_{II}$	$\Gamma_{mig,WS_{II}}(i) = \Gamma^0_{mig,WS_{II}}(i)w_i \sum_{j\neq i}(1-s_j)\exp\left\{-\beta\left[E^0_{a,WS_{II}} + PBJ\right]\right\}$	1.1×10^{12} (Γ^0), 9.647 (E^0)	2.06×10^{12} (Γ^0)	1.67×10^{12} (Γ^0) [1.62, 1.72] $\times 10^{12}$ ‡
8. S_{II} → W migration	$BS_{II} + W \rightarrow S_{II} + BW$	$\Gamma_{mig,S_{II}W}(i) = \Gamma^0_{mig,S_{II}W}(i)s_i \sum_{j\neq i}(1-w_j)\exp\left\{-\beta\left[E^0_{a,S_{II}W} + PBJ\right]\right\}$	0.8×10^{13} (Γ^0), 24.1174 (E^0)	1.97×10^{12} (Γ^0)	2.99×10^{12} (Γ^0) [2.97, 3.01] $\times 10^{12}$ ‡

Here, (Γ^0) identifies the pre-exponential value in units of s^{-1} and (E^0) identifies the value of the activation energy in units of kJ mol^{-1}. "PBJ" stands for the Parabolic Jump Model. *Convention*: $J_{ij} < 0$ for repulsive interactions; $J_{ij} > 0$ for attractive interactions. – Denotes unoptimized base parameters. *Calculated based upon kinetic theory of gases with an assumed sticking coefficient of unity. †Calculated based upon entropic thermodynamic constraint. ‡80% confidence interval calculated for MC optimized parameters.

surface sites rather than bulk-like sites. As a result, here it is just the ratio of adsorption and desorption constants, i.e. the equilibrium constants, which are obtained. We return again to this point below. The fact that 17 possible parameters exist for optimization in this system of single component adsorption, desorption and diffusion, emphasizes the need for a rational approach for parameterizing complex molecular models.

EXPERIMENTAL DATA FOR MODEL TRAINING

Simultaneous parameterization of all adsorption, desorption and diffusion microprocesses is essential for equilibrium as well as gradient simulations (e.g. uptake in zeolite particles and permeation through membranes), where the system dynamics are affected not only by the intrazeolite migration but also by adsorption and desorption at the gas–solid interface. The approach that we adopt in this work is to train the molecular models with experimental data under equilibrium conditions. Specifically, we employ adsorption isotherms and temperature- and loading-dependent PFG-NMR self-diffusivity data to simultaneously fit sensitive parameters of all microprocesses.

Ruthven and Doetsch [23] have studied the equilibrium adsorption of benzene in NaX zeolite with a Si/Al ratio of 1:2. In that work, they compiled multiple adsorption isotherms spanning a substantial temperature range (i.e. 338–513 K). In addition, Germanus *et al.* [24] performed PFG-NMR self-diffusivity measurements of benzene in NaX zeolite of an identical Si/Al ratio. In these studies, they determined self-diffusivity as a function of temperature as well as benzene loading. We employ these various sets of equilibrium data for the purpose of training the molecular model.

MEAN FIELD (MF) MODEL DESCRIPTION

MF models operate upon the assumption of homogeneous spatial distribution of species. They ignore system noise and correlations, which can play a significant role in system properties especially when strong adsorbate–adsorbate forces exist. Yet, their deterministic form makes them amenable to rapid numerical solution as opposed to the alternative computationally intensive molecular simulations. As a result, they can serve as a powerful screening tool (lower hierarchical model) for rapid exploration of parameter space when employed in optimization. Here, we describe MF models employed to calculate adsorption isotherms and self-diffusivity for benzene in NaX zeolite.

MF adsorption isotherms can be derived for benzene in NaX zeolite where lateral interactions between neighboring adsorbates are considered. As a result of the dual-site (i.e. W and S_{II}) nature of this system, two coupled adsorption isotherms arise. Here, we derive the adsorption isotherms based upon kinetics by equating the rates of adsorption and desorption at equilibrium. The resulting MF system of equations describing the fractional benzene coverage on the weak-binding sites (θ_W) and the strong-binding sites ($\theta_{S_{II}}$) is given by

$$\theta_W = \frac{(\Gamma^0_{ads,W}/\Gamma^0_{des,W})P\exp\{\beta[|\varepsilon^0_W| + 6(J_{W,W}\theta_W + J_{W,S_{II}}\theta_{S_{II}})]\}}{1 + (\Gamma^0_{ads,W}/\Gamma^0_{des,W})P\exp\{\beta[|\varepsilon^0_W| + 6(J_{W,W}\theta_W + J_{W,S_{II}}\theta_{S_{II}})]\}}$$
$$\theta_{S_{II}} = \frac{(\Gamma^0_{ads,S_{II}}/\Gamma^0_{des,S_{II}})P\exp\{\beta[|\varepsilon^0_{S_{II}}| + 3(J_{S_{II},S_{II}}\theta_{S_{II}} + J_{S_{II},W}\theta_W)]\}}{1 + (\Gamma^0_{ads,S_{II}}/\Gamma^0_{des,S_{II}})P\exp\{\beta[|\varepsilon^0_{S_{II}}| + 3(J_{S_{II},S_{II}}\theta_{S_{II}} + J_{S_{II},W}\theta_W)]\}}, \quad (1)$$

where β is the Boltzmann factor, $\beta = (kT)^{-1}$, T is the system temperature, P is the system pressure, and θ_i is the fractional loading of the binding site of type i. The factors of 6 and 3 account for the local *interaction* coordination of benzene molecules bound to the W and S_{II} sites, respectively, according to the PES proposed by Ref. [25].

with the thermodynamically derived one

$$K_i = \exp\{\beta(|\varepsilon^0_i| - T\Delta S_i)\}, \quad (4)$$

it is clear that the ratio of the adsorption rate constant to the desorption rate constant captures the entropy change upon adsorption.

In comparing Eqs. (1) and (2), we are reminded of the inherent assumption in our kinetically derived adsorption isotherm of gas ideality. It is important to note, however, that by employing both the Virial [26] and Peng Robinson equations of state, we have found negligible non-ideality over the range of experimental pressures. This suggests that no error should arise from using pressure instead of chemical potential.

For benzene in NaX and NaY, Saravanan and Auerbach [27–29] showed that a MF approximation of the self-diffusivity can be obtained

$$D_{self}(\theta) \cong \frac{(1-\theta_W)\langle\Gamma^0_{WW}\exp(-\beta E_{a,WW})\rangle + (1-\theta_{S_{II}})\langle\Gamma^0_{WS_{II}}\exp(-\beta E_{a,WS_{II}})\rangle}{2[1 + 2(\theta_{S_{II}}/\theta_W)]}\, a^2_\theta \quad (5)$$

by assuming long-range supercage-to-supercage motion (a_θ is the mean intercage jump distance), ignoring fluctuations in the pre-exponentials for migration, expressing the activation energy in terms of the Parabolic Jump Model, and averaging over fluctuations in the activation energies for migration.

A MF isotherm model based upon thermodynamic arguments can likewise be derived where the bulk gas pressure is expressed more accurately in terms of the chemical potential. The isotherm, cast in a form comparable to Eq. (1), is given by

$$\theta_W = \frac{(f(P)/P_0)\exp\{\beta[|\varepsilon^0_W| - T\Delta S_W + 6(J_{W,W}\theta_W + J_{W,S}\theta_{S_{II}})]\}}{1 + (f(P)/P_0)\exp\{\beta[|\varepsilon^0_W| - T\Delta S_W + 6(J_{W,W}\theta_W + J_{W,S_{II}}\theta_{S_{II}})]\}}$$
$$\theta_{S_{II}} = \frac{(f(P)/P_0)\exp\{\beta[|\varepsilon^0_{S_{II}}| - T\Delta S_{S_{II}} + 3(J_{S_{II},S_{II}}\theta_{S_{II}} + J_{S_{II},W}\theta_W)]\}}{1 + (f(P)/P_0)\exp\{\beta[|\varepsilon^0_{S_{II}}| - T\Delta S_{S_{II}} + 3(J_{S_{II},S_{II}}\theta_{S_{II}} + J_{S_{II},W}\theta_W)]\}}, \quad (2)$$

where we have assumed the ideal bulk gas to be the standard state, $f(P)$ is the fugacity of benzene in the gas phase, P_0 is the standard state pressure, and ΔS_i is the change in entropy of adsorption from the bulk gas to the site of type i.

By comparing the kinetically derived Henry's constant

$$K_i = (\Gamma^0_{ads,i}/\Gamma^0_{des,i})\exp(\beta|\varepsilon^0_i|) \quad (3)$$

GRAND CANONICAL AND CANONICAL ENSEMBLE SIMULATIONS

The MF assumption tends to break down for systems where strong adsorbate–adsorbate forces exist. As a result, we have developed a general molecular

modeling toolbox to stochastically simulate such systems. First, a three-dimensional structure-building algorithm capable of generating general zeolite lattices was constructed. Given (1) the coordinates and energetic characteristics of binding sites in a periodic building unit (PBU), (2) pathways for site-to-site migration, and (3) an adsorbate–adsorbate PES, the algorithm constructs computational lattices of arbitrary size and orientation to study equilibrium and dynamics. The flexible lattice-building algorithm is capable of studying systems of finite thickness (e.g. membranes) in addition to infinite domains employing periodic boundary conditions. Finite thickness systems can be modeled via either Dirichlet or Robyn boundary conditions. In the former, the boundary loadings are enforced according to the partial equilibrium assumption. In the latter, the system boundaries participate in adsorption and desorption with the fluid phase and migration with the zeolitic nearest neighboring sites (but not with the fluid).

We have developed a general Monte-Carlo algorithm that is capable of simulating multiple microprocesses (e.g. adsorption, desorption, diffusion, reaction) within the lattice constructed by the lattice-building tool. This Monte-Carlo algorithm falls into the class of continuous time, DMC or KMC simulations reviewed in Ref. [30], which enable real-time tracking of system behavior. The KMC algorithm generally proceeds by calculating the total transition probability per time. Subsequently, a random number is generated and employed to select a microprocess based on the transition probabilities. The general algorithm created here employs a tree structure for improved efficiency in selecting a microprocess. In particular, the total transition probability of each PBU is calculated. Initially, a PBU is selected based upon the PBU transition probabilities and a random number. Subsequently, a site within the chosen PBU is selected based upon the transition probabilities of sites within the PBU. Finally, a microprocess involving this site is randomly chosen. After the execution of a Monte-Carlo event, updates to the local and total probabilities are completed without screening the entire lattice, and the average system time is advanced by the inverse of the total transition probability per unit time.

With this lattice system, we perform lattice GCMC and canonical MC simulations in order to predict adsorption isotherms and self-diffusivity, respectively. In both ensembles, we employ a 3D lattice of binding sites representing a total of 3^3 NaX PBUs (here PBUs consist of four supercages or half of a standard unit cell), and impose periodic boundary conditions in the x, y and z directions. Simulations with all three mechanisms combined are also presented to illustrate thermodynamic consistency issues in real systems where these mechanisms coexist.

Grand Canonical Simulations for Evaluation of Adsorption Isotherms

In order to simulate adsorption isotherms within the grand canonical ensemble, we contact the lattice with a bulk gas at a constant chemical potential, and consider two microprocesses: adsorption and desorption. An adsorption (insertion) of a molecule at a weak (W) and a strong (S_{II}) binding site within the periodic domain is allowed with a transition probability per time given by Eqs. (1) and (3) in Table I, respectively, where w_i and s_i are the order parameters (0 or 1) characterizing the weak (W) and strong (S_{II}) binding site as empty or occupied, respectively. Eqs. (2) and (4) of Table I give the transition probabilities of desorption of a molecule from each type of binding site within the zeolite lattice.

Adsorption isotherms are calculated by natural parameter continuation in pressure. Specifically, the pressure of the contacting gas was incrementally increased, where lattice occupancies at each pressure increment were initialized from the previous solution. Following a discarded equilibration stage of 1×10^4 Monte-Carlo steps (i.e. here a step consists of n MC events, where n is the number of lattice points), statistics were collected for 10^5 Monte-Carlo steps.

Canonical Ensemble Simulations for Evaluation of Self-diffusivity

Self-diffusivity was calculated in the canonical ensemble, where only migration microprocesses (see Eqs. (5)–(8), Table I for transition probabilities) were sampled in the absence of adsorption and desorption. The parabolic jump model, extended by Auerbach and co-workers [11,25,31] to this system from its original surface science applications by Hood *et al.*, [32], is employed to account for the effect of adsorbate–adsorbate interactions on the zero coverage activation energy, $E^0_{a,ij}$.

Loading dependence of the self-diffusivity was determined by initially randomly loading the NaX lattice of binding sites with a specified number of molecules corresponding to the reported experimental loadings. The average supercage-to-supercage distance traversed by diffusing molecules and the average supercage residence time was monitored for convergence following [33,34]. Once convergence was obtained, mean square displacement was extracted from the Einstein relation based upon a multiple time-step, multiple time-origin analysis proposed in Ref. [34], whereby mean square displacement is averaged over all molecules for small time

windows (i.e. a fraction of the mean supercage residence time).

METHODOLOGY FOR ASSESSING THERMODYNAMIC CONSISTENCY OF PARAMETERS IN ENSEMBLES WITH MULTIPLE MICROSCOPIC PROCESSES

In most physical systems, different mechanisms occur simultaneously. For example, during an uptake experiment, adsorption and desorption happen at the gas–solid interfaces whereas diffusion occurs within the bulk. Appropriate parameterization of molecular models consisting of a potentially large number of individual microprocesses within complex microporous materials demands thermodynamic consistency. Thermodynamic consistency not only implies that each microprocess separately obeys microscopic reversibility, but that multiple microprocesses correspond to an identical underlying Hamiltonian.

We illustrate this idea by considering the system of benzene in NaX zeolite. From Table I, the equilibrium constants for the reversible adsorption/desorption steps, as well as the reversible migration steps, are

$$\begin{aligned}
&\mathrm{B} + \mathrm{W} \underset{\Gamma_{\mathrm{des,W}}}{\overset{\Gamma_{\mathrm{ads,W}}}{\rightleftharpoons}} \mathrm{BW} && K_{\mathrm{W}} = \Gamma_{\mathrm{ads,W}}/\Gamma_{\mathrm{des,W}} = (\mathrm{BW})/(\mathrm{B}\cdot\mathrm{W}) \\
&\mathrm{B} + \mathrm{S_{II}} \underset{\Gamma_{\mathrm{des,S_{II}}}}{\overset{\Gamma_{\mathrm{ads,S_{II}}}}{\rightleftharpoons}} \mathrm{BS_{II}} && K_{\mathrm{S_{II}}} = \Gamma_{\mathrm{ads,S_{II}}}/\Gamma_{\mathrm{des,S_{II}}} = (\mathrm{BS_{II}})/(\mathrm{B}\cdot\mathrm{S_{II}}) \\
&\mathrm{BW} + \mathrm{S_{II}} \underset{\Gamma_{\mathrm{migS_{II}W}}}{\overset{\Gamma_{\mathrm{mig,WS_{II}}}}{\rightleftharpoons}} \mathrm{BS_{II}} + \mathrm{W} && K_{\mathrm{WS_{II}}} = \Gamma_{\mathrm{mig,WS_{II}}}/\Gamma_{\mathrm{mig,S_{II}W}} = (\mathrm{BS_{II}}\cdot\mathrm{W})/(\mathrm{BW}\cdot\mathrm{S_{II}}),
\end{aligned} \tag{6}$$

where migration between like sites (W⇋W and S_{II}⇋S_{II}) is not shown since the corresponding equilibrium constants are simply equal to unity. From this kinetics approach, it is clear that benzene adsorption/desorption is coupled to the migration between the binding sites via the ratio of equilibrium constants,

$$\begin{aligned}
K_{\mathrm{WS_{II}}} &= K_{\mathrm{S_{II}}}/K_{\mathrm{W}} \\
&= (\Gamma_{\mathrm{ads,S_{II}}}/\Gamma_{\mathrm{des,S_{II}}})(\Gamma_{\mathrm{des,W}}/\Gamma_{\mathrm{ads,W}}) \\
&= \Gamma_{\mathrm{mig,WS_{II}}}/\Gamma_{\mathrm{mig,S_{II}W}}.
\end{aligned} \tag{7}$$

Here, we employ the kinetic theory of gases to describe the rate of adsorption of a molecule to site $i = \mathrm{S_{II}}$ or W,

$$\Gamma_{\mathrm{ads},i} = (\rho_{\mathrm{site},i}\rho_{\mathrm{sat}})^{-1}(s_{0,i}PN_{\mathrm{A}})(2\pi MRT)^{-1/2}, \tag{8}$$

where $s_{0,i}$ is the sticking coefficient, N_{A} is Avogadro's number, $\rho_{\mathrm{site},i}$ is the density of the sites of type i within the lattice, ρ_{sat} is the saturation density (molecules/site), M is the molecular weight of the adsorbing molecule, and R is the ideal gas constant. The sticking coefficient is included to capture the steric hindrance and/or indirect surface diffusion [35,36] limiting the number of molecular trajectories resulting in micropore adsorption. As mentioned above, it is only surface sites that are involved in adsorption and desorption, but this fact does not affect the equilibrium constants computed here.

By algebraic manipulation of the equilibrium constants, we derive the following constraints governing thermodynamic consistency of this system in the limit of zero coverage

$$\begin{aligned}
&(s_{0,\mathrm{S_{II}}}/s_{0,\mathrm{W}})(\Gamma^0_{\mathrm{des,W}}/\Gamma^0_{\mathrm{des,S_{II}}})(\rho_{\mathrm{site,W}}/\rho_{\mathrm{site,S_{II}}}) \\
&\quad = \Gamma^0_{\mathrm{mig,WS_{II}}}/\Gamma^0_{\mathrm{mig,S_{II}W}} \qquad (9) \\
&\quad |\varepsilon^0_{\mathrm{W}}| - |\varepsilon^0_{\mathrm{S_{II}}}| = E^0_{a,\mathrm{WS_{II}}} - E^0_{a,\mathrm{S_{II}W}}. \qquad (10)
\end{aligned}$$

Given the relationship between pre-exponentials and entropy change upon adsorption Eqs. (3) and (4), it is clear that the first constraint, Eq. (9), governs entropic consistency while the second one, Eq. (10), governs enthalpic consistency of the system. In simple words, Eqs. (9) and (10) imply that one cannot simply arbitrarily choose the pre-factors and activation energies of adsorption, desorption and migration processes. For example, use of a Langmuir isotherm that describes experimental data and the Maxwell-Stefan transport framework trained from independent molecular modeling could lead to a fundamentally inconsistent membrane model. We illustrate the implications of thermodynamic inconsistency below.

In general, a rational approach [37] for determining the number of degrees of freedom in arbitrarily complex systems is to evaluate the number of adsorbed species and microscopic processes cast as reversible reactions, and construct the reaction matrix of stoichiometric coefficients of the species in the system of reversible reactions. By evaluating the rank of this matrix (degrees of freedom), one can identify the number of linearly independent reactions (or microscopic processes here) and subsequently evaluate the equilibrium constants of the dependent reactions from the independent ones.

It is important to note that thermodynamic consistency is potentially fortuitously achieved for simple systems consisting of a single guest species on a lattice of identical binding sites. In such cases, the migration equilibrium constant is equal to unity (i.e. entropic and enthalpic changes upon migration in the zero coverage limit are zero). As a result, by ensuring thermodynamic consistency of the individual microprocesses, a simple task, the overall system is also thermodynamically consistent.

Implications of Thermodynamic Inconsistency under Equilibrium Conditions

Figures 2 and 3 show the effect of thermodynamic inconsistency under equilibrium conditions. We employ GCMC simulations to calculate adsorption isotherms in the presence and absence of site-to-site migration. Since equilibrium is unique, the inclusion of site-to-site migration in GCMC simulations should not alter the unique loading distribution of benzene between the two types of binding sites.

We first consider a thermodynamically consistent (TC) case in which the diffusion parameters and energetics are taken from a consistent literature model [25] satisfying the enthalpic constraint, Eq. (10). The adsorption model is then parameterized by fitting the pre-exponential of desorption of benzene from the W site, and calculating the pre-exponential of desorption from the S_{II} site based upon the entropic constraint, Eq. (9). As such, entropic consistency is also enforced. Figure 2 shows the poor qualitative agreement of the adsorption isotherm in comparison to the experimental data of [23] as a result of independently fitting the experimental data. While such poor model prediction could be attributed to other reasons, it is our experience from modeling various systems that this is typically caused by the unoptimized parameters rather than fundamental limitations of the model itself. We illustrate this point below. Figure 3 compares the equilibrium loading of the W and S_{II} sites at two pressures (one from the high- and one from the low-pressure solution branches, shown in Fig. 2 as P_{high} and P_{low}, respectively) calculated via the GCMC algorithm with and without migration. Despite the inability of the model to capture the adsorption isotherm, it at least does not alter the distribution of adsorbates between sites (manifested by the identical loading distribution obtained with and without migration in Fig. 3).

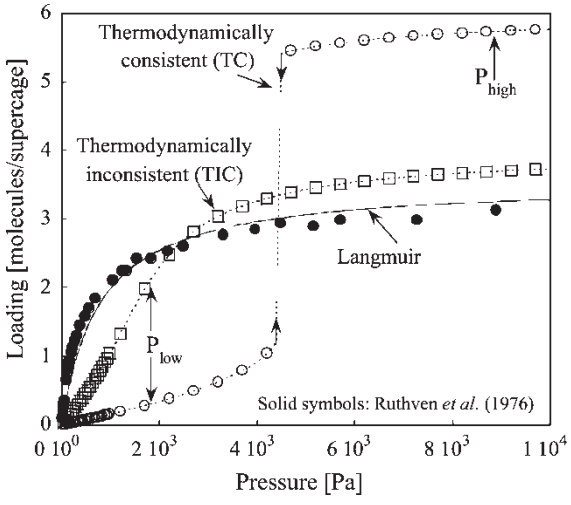

FIGURE 2 Illustration of various MF fitted adsorption models in comparison to an experimental adsorption isotherm of benzene in NaX at 513 K (solid symbols). The thermodynamically consistent (TC) isotherm obeys both entropic and enthalpic consistency, whereas the TIC isotherm is entropically inconsistent. A fitted Langmuir isotherm is also shown. The arrows denote the high (P_{high}) and low (P_{low}) pressures corresponding to the loading distribution analysis in Fig. 3.

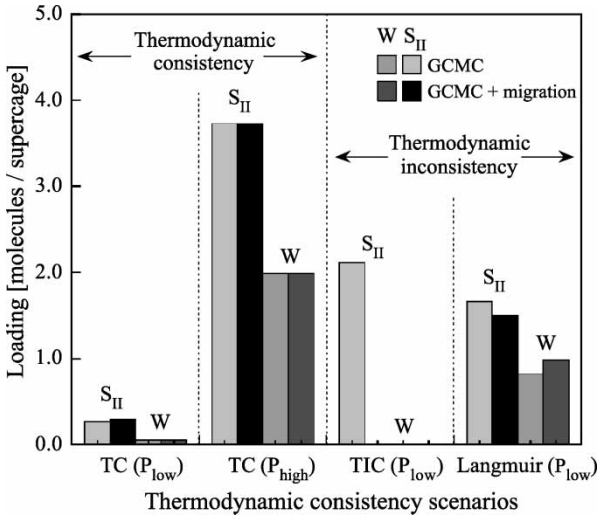

FIGURE 3 Loading distribution in terms of molecules/supercage between the strong (S_{II}) and weak (W) binding sites corresponding to the model isotherms presented in Fig. 2. Distributions from both the high- and low-pressure adsorption branches (P_{high} and P_{low} in Fig. 2) for the thermodynamically consistent (TC) model are shown, whereas loadings at P_{low} are shown for the thermodynamically inconsistent (TIC) and Langmuir models. Differences in loading for the same type of site upon including migration result from thermodynamic inconsistency.

If the entropic constraint is relaxed (Case: TIC), through simultaneous adjustment of the pre-exponentials of desorption from the W and S_{II} sites, the adsorption isotherm fit to the experimental data is improved, as depicted in Fig. 2. Yet the fundamental violation of thermodynamic consistency is apparent when simulations of adsorption isotherms are conducted in the presence of site-to-site migration. The GCMC equilibrium solution obtained with only adsorption and desorption, depicted in Fig. 3, shows a moderate molecular loading of only the S_{II} sites. By turning on site-to-site migration, the lattice empties in a dramatic misprediction of W and S_{II} loading distribution as a result of violations of entropic consistency.

It is standard practice in the literature to capture experimental adsorption isotherms using a single-site Langmuir isotherm. Such isotherms are derived for ideal systems, where adsorbate–adsorbate interactions are not considered. In Fig. 2, we show that a good fit of the experimental isotherm is indeed obtained using a single-site Langmuir form (Case: Langmuir). Since the single-site Langmuir model assumes only one type of site, and, thus, an identical characteristic heat of adsorption for both the S_{II} and W sites, it results in violation of enthalpic consistency, Eq. (10), for a system where adsorption, desorption, and diffusion take place simultaneously. By a similar argument, the single-site Langmuir framework also violates entropic consistency. The effect of the fundamental violation of both constraints on thermodynamic consistency is shown in Fig. 3. We observe that a non-unique loading distribution is predicted in the presence and absence of site-to-site migration.

Although the effects of thermodynamic consistency under equilibrium conditions were evaluated here, similar effects are conceivable in predicting permeation properties in gradient systems or site-specific reaction rates in reaction-diffusion systems. Furthermore, larger discrepancies than the Langmuir example presented here are obviously possible.

HIERARCHICAL APPROACH TO MOLECULAR MODEL PARAMETERIZATION

Based on the above discussion, it is clear that thermodynamic consistency is key to successfully parameterizing molecular models of systems with multiple microprocesses. Furthermore, we show in Appendix A that fitting models to limited sets of experimental data can hinder the robustness of the optimized model. As a result, the approach we adopt seeks a physical set of parameters that optimizes the model response to multiple sets of disparate experimental data (e.g. adsorption isotherms and PFG-NMR self-diffusivity data). For this purpose, a joint objective function,

$$f = \sum_{k}^{N} \left[\Phi_k \sum_{i}^{n(k)} \phi_i (1 - x_i / x_i^{\exp})_k^2 \right], \qquad (11)$$

is minimized that compares the model response, x_i, to N sets of potentially disparate experimental data, $x_i^{\exp}$, where uncertainty in each data point and data set is enforced through the respective weightings ϕ_i and Φ_k. Here $n(k)$ is the number of points in data set k.

Most physical systems of interest exhibit a plethora of local minima. It is, therefore, important to employ techniques that have a large probability of finding the global minimum. Genetic algorithms and simulated annealing are two such approaches. Here we employ the latter. Simulated annealing requires solution of the full model at each function call of the algorithm (e.g. as many as $\sim 10^7$ function calls for a slow simulated annealing optimization). Recognizing the CPU required for generation of adsorption isotherms and convergence of self-diffusivity calculations, both on the order of approximately 1 CPU hour, it is obvious that direct optimization of even a single parameter of a molecular model is computationally infeasible.

Therefore, we propose a rational hierarchical approach towards parameterization of molecular models. One starts with MF models whose rapid solution makes them amenable to extensive search in parameter space via global optimization type of techniques. Recognizing the limitations of MF models, however, we treat the identified parameter set simply as good initial guesses for the parameterization of the molecular models.

Yet even with a good initial guess of parameters, the computational cost of molecular models still deems direct global optimization infeasible. Therefore, the final step in the hierarchical scheme used in this work is to employ surface response techniques for optimization of the parameters of molecular models. In particular, given a relatively narrow parameter space identified using the MF optimized parameters, we turn to factorial design methods to minimize the number of molecular simulations required to develop an approximate model response surface. Direct simulated annealing of this surface results in rational training of the molecular models. We illustrate the various steps below.

Base Parameterization of MF Models

In order to perform simulated annealing optimization of the MF model parameters, a starting parameter set is needed. It seems only rational to at least parameterize the diffusion model from the work of Auerbach and co-workers [25]. These parameters are shown in column 4 of Table I and column 2 of Table II. In general, the zero-coverage

TABLE II Summary of energetic base and optimized parameters in units of kJ mol^{-1}

Energetic parameter	*Base parameters*	*MF optimized parameters*	*MC optimized parameters*
1. ε_W^0	−60.78	–	–
2. $\varepsilon_{S_{II}}^0$	−75.25	–	–
3. $J_{WS_{II}} = J_{S_{II}W}$	2.89	−1.85	−1.55 [−1.63, −1.47]*
4. J_{WW}	2.89	−10.53	−13.05 [−14.24, −11.85] *
5. $J_{S_{II}S_{II}}$	2.89	−3.29	−2.95 [−3.14, −2.77] *

Convention: $J_{ij} < 0$ for repulsive interactions; $J_{ij} > 0$ for attractive interactions. – Denotes unoptimized base parameters. *80% confidence interval calculated for MC optimized parameters.

site-to-site migration activation energies were extracted from the Germanus *et al.* [24] data. Furthermore, the heats of adsorption for benzene on the W and S_{II} sites were determined from experiment [25,34,38,39].

The parameters of most marked uncertainty are the pre-exponentials for site-to-site migration as well as the adsorbate–adsorbate forces. The pre-exponentials were calculated for benzene in NaY via transition state theory (TST) and reactive flux correlations, and were adjusted for dynamical corrections [40–42]. The difficulty in properly locating the dividing surface in TST calculations [42] makes these parameters uncertain.

The adsorbate–adsorbate coupling parameters, J_{ij}, were assumed to be equal for all pairs of interactions of benzene molecules located at neighboring binding sites (i.e. W⇋W, S_{II}⇋W, S_{II}⇋S_{II}). A single value describing these interactions as attractive was extracted from the second virial coefficient of the heat of adsorption [31,39]. It should be noted, however, that the extraction of the intermolecular coupling parameter assumes temperature independence of the isosteric heat of adsorption. Such an assumption may not be satisfied in light of the two types of binding sites, with the isosteric heat of adsorption being a loading dependent combination of the heat of adsorption of each site. An illustration of the uncertainty of these parameters is explored in Appendix B. A nominal pre-exponential for desorption from the window (W) site was assumed to be $10^{13}\,s^{-1}$, based upon the standard vibrational frequency employed in surface science studies. Using the entropic thermodynamic constraint, Eq. (9), the pre-exponential for desorption from the S_{II} site was calculated.

The base (unoptimized) MF model response in comparison to the experimental data is shown in Figs. 4 and 5 (dotted lines). Significant over prediction of the saturation loading in comparison to the experimental one is observed. Furthermore, although the activation energy of the self-diffusivity is captured relatively well, the unoptimized self-diffusivity over predicts the experimental values by more than one order of magnitude. Even more interesting is the fact that the self-diffusivity at the higher loadings is predicted to be greater than that at the lower loadings. These deviations could be attributed to the limitations of the MF model or the model parameters. We discuss the inherent limitations of lattice models and MF later. Yet, as illustrated below and found in many examples from our work on development of complex surface kinetic mechanisms, such deviations are very common to models with unoptimized parameters.

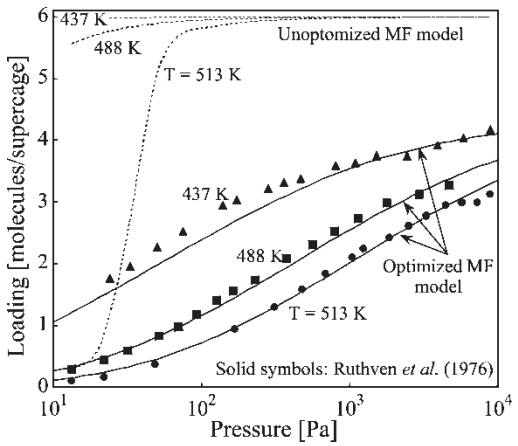

FIGURE 4 Comparison of the unoptimized (dotted lines) and optimized (solid lines) MF adsorption response to experimental adsorption isotherms at three temperatures.

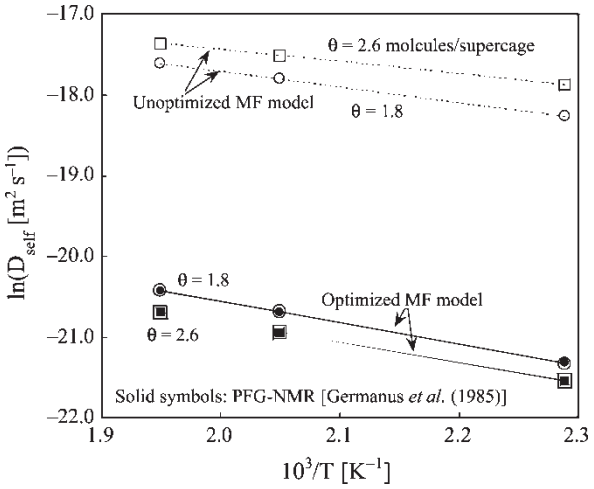

FIGURE 5 Arrhenius plot comparing the self-diffusivity predicted via the unoptimized (open symbols, dotted line) and optimized (open symbols, solid line) MF model response to the experimental PFG-NMR self-diffusivity data (solid symbols) employed in the optimization. Simultaneous optimization was completed for two supercage loadings (1.8 and 2.6 molecules/supercage), each at the temperatures shown.

Identifying Sensitive Parameters for Optimization of MF Models

Given the relative confidence in the activation energies of migration and heats of adsorption at zero-coverage, these values were fixed. Due to the over prediction of the saturation loading with the base adsorbate–adsorbate interaction parameters, and their relative uncertainty, we include $\{J_{ij}\}$ in the optimization list. In order to identify which other parameters are important to refine, brute-force local sensitivity analysis was done. Fig. 6 identifies the model sensitivity to perturbations in the equilibrium constants for the reversible adsorption/desorption steps as well as migration steps. The perturbation of the equilibrium constants was small (−0.01%) in order to maintain relative thermodynamic consistency.

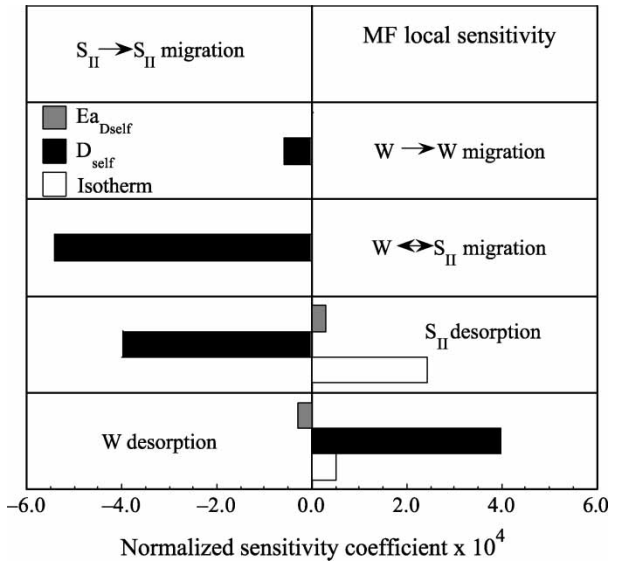

FIGURE 6 Normalized sensitivity coefficients of the self-diffusivity, its apparent activation energy, and the adsorption isotherm behavior to small perturbations (−0.01%) of the equilibrium constants associated with the reversible microprocesses of adsorption/desorption and site-to-site migration. Only parameters with high sensitivity are selected for optimization.

As a result of the functional form of the self-diffusivity, the model was insensitive to the $S_{II} \rightleftharpoons S_{II}$ migration and relatively insensitive to the $W \rightleftharpoons W$ migration rate. Of the five reversible processes, the MF model response was most sensitive to the $W \rightleftharpoons S_{II}$ migration rate, and the S_{II} and W desorption rates. Therefore, we concluded that the pre-exponential parameters to which the model was most sensitive were, $\Gamma^0_{mig,WS_{II}}$, $\Gamma^0_{mig,S_{II}W}$, $\Gamma^0_{des,W}$, and $\Gamma^0_{des,S_{II}}$. Assuming unity sticking coefficients for adsorption, it is clear that only three of these four parameters can be optimized according to the entropic constraint, Eq. (9), discussed previously. The S_{II} desorption pre-exponential, $\Gamma^0_{des,S_{II}}$, was calculated based on thermodynamic consistency. As a result, a total of six parameters were selected for optimization, ($\Gamma^0_{mig,WS_{II}}$, $\Gamma^0_{mig,S_{II}W}$, $\Gamma^0_{des,W}$, J_{WW}, $J_{WS_{II}}$, and $J_{S_{II}S_{II}}$).

It is important to note that the equilibrium nature of experimental adsorption data limits the extractable information to equilibrium constants (i.e. relative rates) rather than absolute rate constants for adsorption and desorption. In particular, we assume that the sticking coefficients are unity. Therefore, the S_{II} and W desorption rate constants reported here provide insight into equilibrium partitioning rather than absolute rates of desorption. Such insight is invaluable in subsequent investigation of non-equilibrium systems when partial equilibrium boundary conditions are enforced. Ideally, however, one would like to also train the model with transient experimental data (e.g. uptake experiments performed with zeolite pellets) to fix the absolute magnitude of these rate constants (i.e. extract sticking coefficients for these systems) so that dynamics of non-equilibrium systems could be quantitatively studied. The characteristic length and time scales of transient experimental systems, however, prohibit their direct molecular simulation, and alternative multiscale approaches based on coarse-grained Monte-Carlo [43–45] or mesoscopic theories [46–48], for example, must be employed for obtaining absolute rate constants.

Deterministic Numerical Methods Employed in Solving MF Models and Optimized MF Results

For benzene in NaX, we employ the MF adsorption isotherms, Eq. (1), and self-diffusivity models, Eq. (5). In general, wide bounds were placed upon the sensitive pre-exponential parameters within the annealing algorithm. At each optimization step, three adsorption isotherms were generated at three experimental temperatures using Newton's method. Due to the relatively large bounds placed upon the parameters being optimized and the stochasticity of the simulated annealing approach, regions of parameter space were explored that severely challenged Newton's convergence. As a result, we also employed the DLSODA [49,50] package to compute pseudo-transients that lead towards steady state to aid convergence of Newton's method. In other words, we employ a hybrid steady state/transient solver to obtain solutions. Furthermore, Newton's method was used to identify the pressure and the loading distribution between the W and S_{II} sites corresponding to the experimental benzene loading for the self-diffusivity data.

In light of the desire to dramatically improve the prediction of the saturation loading from the base case, extra weight was given to the saturation adsorption isotherm points during optimization. The MF optimized parameters are tabulated in Tables I and II. The predicted MF adsorption isotherms and self-diffusivity are depicted in Figs. 4 and 5, respectively. Considerable improvement of the model response to both sets of data was achieved. With the optimized parameters, the model now captures well the saturation loading and temperature dependence of adsorption as well as the activation energy and magnitude of the self-diffusivity.

Surface Response Techniques for Molecular Model Parameterization

With trained MF models, we turn now to the parameterization of molecular simulations. It is interesting to first calculate the MC model response with the MF optimized parameter set to assess how good the MF parameters are as an initial guess for the full stochastic molecular model. Figures 7 and 8

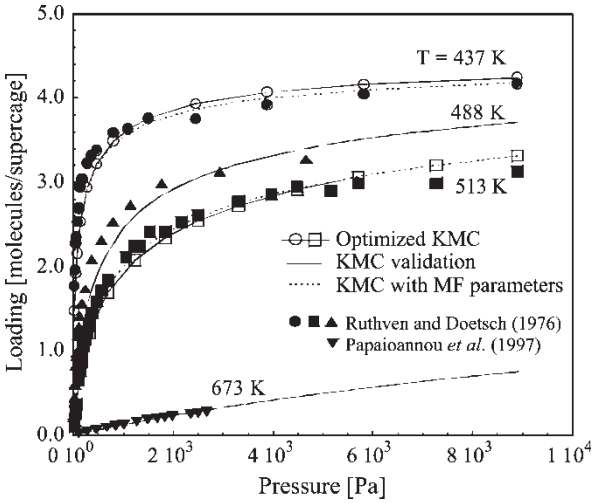

FIGURE 7 Benzene experimental adsorption isotherms in units of molecules/supercage at 437 K (solid circles) and 513 K (solid squares) compared to KMC isotherms employing (1) the MF optimized parameter set (dotted lines) and (2) the parameter set resulting from three iterative refinements of the model response surface (solid lines, open symbols). Experimental adsorption isotherms not employed in the optimization at 488 K (solid, upright triangles) and 673 K (solid, downward triangles) are shown for validation, where the solid line is a smooth fit of the corresponding KMC isotherms calculated with the surface response optimized parameter set.

show the KMC model response with the MF optimized parameter set for both the adsorption isotherms (dotted lines) and self-diffusivity (open symbols, dotted lines), respectively. The KMC model appears relatively well behaved with the MF optimized parameter set. In particular, the agreement

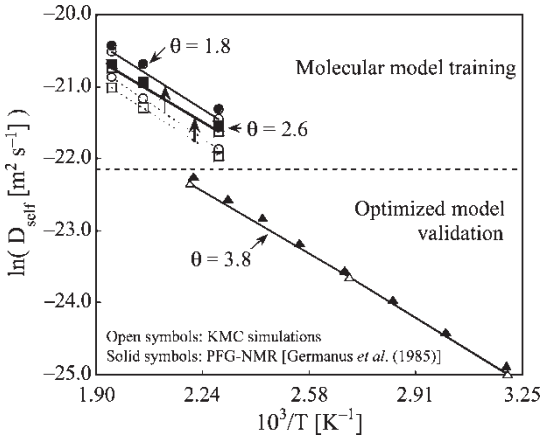

FIGURE 8 Depiction of the PFG-NMR self-diffusivity of benzene in NaX at two loadings (molecules/supercage): 1.8 (solid circles) and 2.6 (solid squares) used for molecular model training, as compared to the self-diffusivity calculated via the KMC model parameterized with (1) the MF optimized parameter set (open symbols, dotted lines) and (2) the optimized parameters from three iterative surface refinements in the surface response approach (open symbols, solid lines). The bold arrows depict the improvement in the self-diffusivity after three surface response iterations. The validation regime compares the PFG-NMR self-diffusivity for a higher loading of 3.8 molecules/supercage (solid triangles) to the trained KMC model prediction (open triangles, solid line).

with the experimental adsorption isotherms is striking, even in light of the underprediction of the self-diffusivity. The MF model of self-diffusivity is unable to capture the exact stochastic system behavior, with deviations observed in the magnitude of the KMC self-diffusivity and activation energies. Next, we describe a rational approach employed for optimization of the molecular models.

Surface response techniques [51] provide a rational alternative to the enormous computational cost associated with direct parameter optimization of expensive models. In this approach a limited number of full molecular simulations are carried out for specific parameter combinations. The collected model response is captured via low (i.e. second) order polynomials, which form a multidimensional response surface. This response surface approximates the model response over the parameter space, and its accuracy is greatest for relatively small parameter spaces. Rigorous simulated annealing optimization can then be applied directly to this surface in order to optimize the model parameters. Since the accuracy of the surface is dependent upon how tightly defined are the ranges for the fitted parameters, an iterative improvement may be required, as suggested in Ref. [52], whereby parameter bounds can be modified to better capture the model response. Another benefit beyond computational speed-up is the fact that these response surfaces allow for optimization to quite different sets of data, by simply adding them to the objective function (Eq. (11)) so that simultaneous fitting can be carried out. Although a standard technique for expensive deterministic models, its use for molecular simulations has only recently been proposed [18].

Following definition of relatively narrow parameter ranges, we have employed two-level, fractional factorial design techniques [51] to ascertain all parameter combinations required to generate the response surface. In the two-level approach we normalize the active pre-exponentials and J_{ij} parameters by the range of sampling, such that the maximum and minimum bounds to the parameter ranges are mapped to $x = +1$ and $x = -1$, respectively. The difference in the parameter types requires geometric normalization of pre-exponentials and arithmetic normalization of the interaction energies. Under full two-level factorial design we would perform sets of molecular simulations for all combinations ($2^6 = 64$) of the maximum and minimum parameter values. As a result of the multiple sets of experimental data fitted, each parameter combination is associated with six molecular simulations (i.e. two adsorption isotherms and four self diffusivity calculations at two temperatures and two loadings), resulting in a total of 384 molecular simulations required for full factorial design. Under fractional factorial design, we systematically

eliminate [51] half of the parameter combinations from full factorial design to further minimize the number of molecular simulations.

Three iterative refinements of the parameter ranges were carried out to improve the accuracy of the response surface so as to avoid convergence of parameters to either the maximum or minimum parameter bound. The MC optimized parameters and confidence intervals are presented in Tables I and II. Figure 7 shows that the adsorption isotherms were relatively insensitive to iterative improvements in the response surface. The magnitude and activation energies of the self-diffusivity, however, did improve considerably as shown by comparing the KMC-predicted self-diffusivity (solid lines, open symbols) with the experimental data at loadings of 1.8 and 2.6 molecules/supercage in Fig. 8.

DISCUSSION OF OPTIMIZED PARAMETERS

In general, the magnitude of both the MF and MC optimized parameters tabulated in Tables I and II appears to be physically reasonable. The optimized pre-exponentials are both within an order of magnitude of standard frequencies expected from surface science studies, and the adsorbate–adsorbate interactions are of a physically realistic order of magnitude. By comparing the optimized and base (unoptimized) parameters, we immediately see the benefit of MF screening for rapidly exploring parameter space. While the MF, MC and base pre-exponentials fall within less than an order of magnitude of one another, more marked differences are observed for the adsorbate–adsorbate interactions. Only fractional deviations exist between the optimized MF and MC interaction parameters. Yet the optimized parameters suggest a distribution of strong and weak repulsions between neighboring benzene molecules within the NaX lattice, whereas the base parameterization was one of equivalent attractive forces.

A point that deserves discussion is the sign of the interactions and their physical meaning. As discussed previously, considerable uncertainty exists in the strength of the reported adsorbate–adsorbate interactions. In particular, Auerbach and co-workers determined, using the second virial coefficient, attractive interactions. On the other hand, Ruthven *et al.* [53] concluded, using a statistical adsorption model to the same isotherm data, strong repulsive interactions even at low loading. In order to understand these differences, we have computed the second virial coefficient of the heat of adsorption (see Appendix B). We have observed either attractive or repulsive effective benzene–benzene forces, depending on what fraction of the isotherms is fitted.

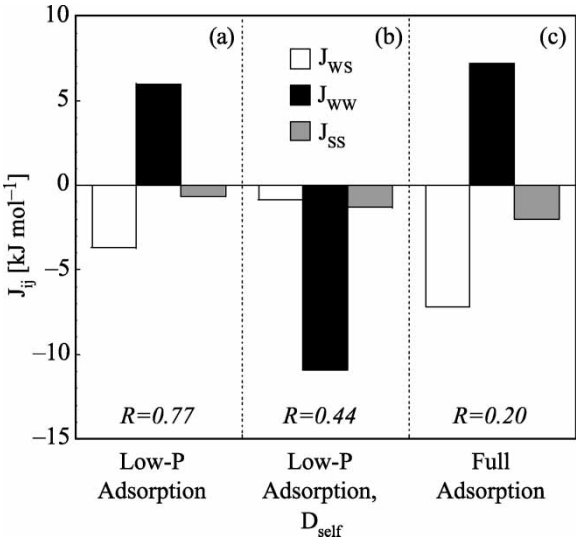

FIGURE 9 Sensitivity of the fitted adsorbate–adsorbate interaction parameters to the portion of the adsorption isotherms and data fitted for three cases: (a) fitting of only the lowpressure portion of the adsorption isotherms, (b) fitting of the low-pressure portion of the adsorption isotherms and the self-diffusivity data simultaneously, and (c) fitting of only the full adsorption isotherms. The residual, *R*, for each case was calculated between the model response and experimental adsorption data over the full range of pressures.

Our approach of extracting the interaction parameters differs from the conventional ones. Since the full isotherms were employed to train the model parameters, it is interesting to briefly investigate whether the saturation loading drives the MF optimization towards the effective repulsive forces. In Fig. 9, we evaluate the sensitivity of the parameters for several cases in which different portions of the experimental data were used for MF training: (a) only the low-pressure adsorption data (i.e. neither the saturation loading nor the self-diffusivity), (b) the low-pressure adsorption data and the self-diffusivity data, and (c) only the full adsorption isotherms (i.e. no self-diffusivity). We observe that while the parameterization is blind to the saturation loading and self-diffusivity data (Fig. 9a), the MF optimization results in a mixture of attractive and repulsive forces. Relative insensitivity of the extracted parameters to the portion of the adsorption isotherm used in the parameterization (i.e. exclusion or inclusion of saturation data) is observed in comparing panels (a) and (c) of Fig. 9. Comparable attractive and repulsive forces are also obtained when the high-pressure (i.e. saturation) loading data is included in the optimization. Finally, panel (b) of Fig. 9 and the parameters extracted through simultaneous optimization against all data (Table II), reveal that the self-diffusivity data, rather than the saturation loading, forces the W–W adsorbate–adsorbate interactions to be repulsive. Given the well-known limitations of MF models, we have also exploited direct optimization of

the molecular model without invoking prior MF training (not shown). We have found that the signs in the first iteration of the surface response are consistent with the ones reported here. It appears that the sign of interactions is not a result of the MF model but most probably a consequence of the lattice model.

The physical significance of the effective repulsive forces is unclear. Such *effective* repulsive forces could conceivably result from confinement effects within the zeolite, where the interactions, unlike those in the bulk gas phase, are complex functions of direct adsorbate–adsorbate and indirect lattice-mediated interactions. Perhaps more probable is the notion that such *effective* repulsive forces arise as a result of the rigid lattice framework. Work within the literature [54–59] has tracked the details of lattice vibrations as well as the propensity for cation (i.e. binding site) migration with changes in system temperature, adsorbate loadings and pressure. These dynamic processes stand to alter the PES for a molecule adsorbed or migrating within a zeolitic pore or supercage, leading to potential migration, creation, or annihilation of binding sites. The rigid lattice model cannot explicitly capture such lattice flexibility and cation migration, yet it is conceivable that the repulsive forces serve to capture this effect. The trained lattice model is able to quantitatively track, but in an effective manner, the experimental adsorption and self-diffusivity data over a range of adsorbate loadings and system temperatures.

VALIDATION OF MODEL PARAMETERIZATION

It is desirable to evaluate the validity of the trained molecular models—for example, by simulating sets of experimental data not used in the optimization procedure. For the adsorption isotherms, we perform two additional simulations. The first simulation with the trained molecular model is conducted for a temperature of 488 K. This is, perhaps, the easiest test for the model, as the optimization was done against experimental isotherms that bounded this isotherm (i.e. $T = 437$ and 513 K). The resulting isotherm predicted by the trained molecular model is shown as the solid line passing through or near the experimental data (solid upright triangles) in Fig. 7. In addition, extrapolation to high temperatures serves as a more stringent test for the validity of the parameterization. To this end, we employ the trained molecular model to calculate the adsorption isotherm at 673 K and compare to the high-temperature data of Papaioannou *et al.*, [60]. Excellent agreement between the model prediction (solid line) and low-pressure experimental data (solid, inverted triangles) is observed in Fig. 7.

Finally, we perform self-diffusivity calculations for a relatively high loading of 3.8 molecules/supercage and over a relatively wide temperature range (i.e. 312–455 K). The resulting excellent agreement of both the activation energy and magnitude of the self-diffusivity (solid line, open triangles) in comparison to the experimental data (solid triangles) is depicted in the validation portion of Fig. 8.

CONCLUSIONS

Motivated by the exorbitant computational cost of directly optimizing molecular models to experimental data, we have presented a hierarchical framework towards rational parameterization of molecular models. This framework employs mean field (MF) models to identify sensitive parameters that are rapidly optimized using global optimization-based techniques. This MF optimum parameter set is subsequently used as an initial guess for molecular models, and surface response techniques are employed to minimize the number of computations required to generate a model response surface. Direct simulated annealing optimization of this surface to multiple, disparate sets of experimental data (e.g. adsorption isotherm and PFG-NMR self-diffusivity data) is possible, and results in efficient training of the molecular models.

We have illustrated the power of this approach to rationally parameterize a molecular lattice model of benzene in NaX zeolite. Guided by both entropic and enthalpic constraints, we have developed a thermodynamically consistent molecular model, capable of capturing the behavior of the real system even when extrapolating beyond the optimization space despite the recognized limitations of lattice models. Exciting possibilities now exist to employ this equilibrium-trained molecular model for gradient calculations where, for example, a consistent parameterization of adsorption, desorption, and diffusion is essential for predicting permeation properties of thin, oriented microporous membranes. Rigorous studies of such membrane systems without the limiting assumption of partial equilibrium at the boundaries, however, demand a level of detail beyond the equilibrium constants extracted in this work. In particular, absolute rates of adsorption and desorption must be determined, potentially by a hierarchical approach employing techniques such as coarse-grained Monte-Carlo [43–45] or mesoscopic theories [46–48] to extract information from larger length and time scale transient experimental studies (e.g. uptake) that are inaccessible to microscopic Monte-Carlo techniques. Such studies of permeation through realistic membranes will be discussed in a forthcoming publication.

Admittedly, the physical significance of some of the extracted parameters (i.e. *effective* repulsive adsorbate–adsorbate forces) is not transparent at the level of coarse-graining involved in lattice models. An explanation of the detailed phenomenon that they capture can and has been conjectured, but models that describe lattice flexibility and binding site migration would be required for direct evidence of the role of lattice dynamics. Along these lines, although we have focused on the illustration of the hierarchical approach and derivation of enthalpic and entropic constraints on a molecular lattice model, it is important to emphasize the broad applicability of this rational approach to all molecular models, including molecular dynamics and atomistic Monte-Carlo simulations. In such instances where MF models do not exist or are not very accurate, the surface response techniques could be applied for direct parameterization of the molecular models to disparate sets of experimental data. The persistent computational savings, albeit less than those with initial MF screening, and rational parameterization to multiple sets of data, emphasize the power of this technique for development of robust molecular and multiscale models.

Acknowledgements

This work has been supported in part by NSF/ITR DMS-0219211. In addition, the authors express their gratitude for useful discussions with Prof. Scott Auerbach.

APPENDIX A: AN EXAMPLE OF FITTING TO A SINGLE SET OF EXPERIMENTAL DATA

It is interesting to consider the possible error incurred where only one type of data is used to train the models rather than simultaneously fitting multiple sets of data. The effect of fitting a model to only the adsorption isotherms, and subsequently attempting to predict the self-diffusivity data, is shown in Figs. 10 and 11. In particular, we employ the same optimization procedure described above against adsorption isotherm data, and fit both pre-exponentials for desorption. Subsequently, the ratio of the migration pre-exponentials (i.e. the equilibrium constant) is corrected to satisfy the entropic constraint. While the resulting fit to the adsorption isotherms is excellent, the prediction of the self-diffusivity is poor regarding both activation energies and magnitudes of the self-diffusivity, especially at lower temperatures. This underscores the need for simultaneous fitting of multiple sets of experimental data describing the underlying microprocesses.

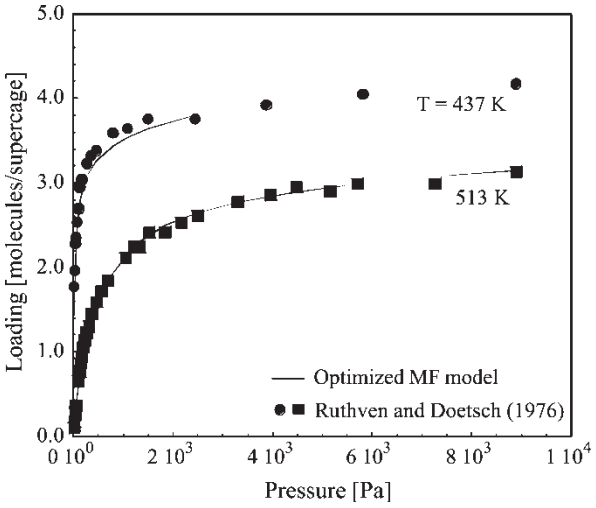

FIGURE 10 MF fitted adsorption isotherms (solid lines) obtained from fitting of the lattice model to the experimental adsorption behavior at 437 K (solid circles) and 513 K (solid squares).

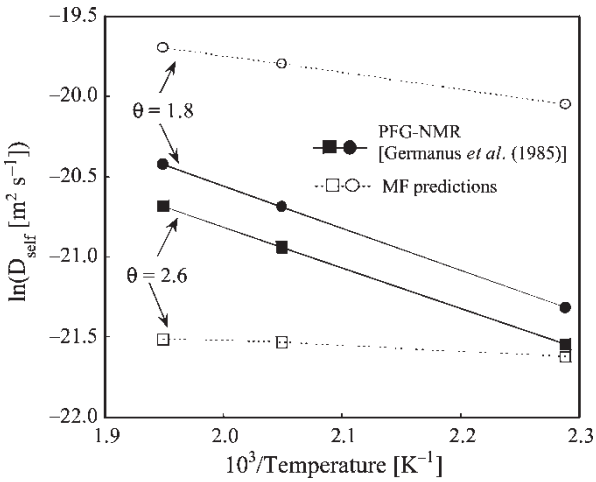

FIGURE 11 Arrhenius plot comparing the MF self-diffusivity (open symbols, dotted lines) predicted from MF fitting of only the experimental adsorption isotherms (Fig. 10) to the temperature-dependent experimental PFG-NMR self-diffusivity data (solid symbols and lines) at two supercage loadings.

APPENDIX B: INHERENT UNCERTAINTY IN THE EFFECTIVE ADSORBATE–ADSORBATE FORCES

A wide range of models has been employed within the literature to describe the adsorption of molecules within microporous materials ranging from virial coefficient approaches [38,39,61,62] to statistical models [53]. The base parameterization [25] of the lattice model employed in this study used attractive adsorbate–adsorbate forces derived from the second virial coefficient of the heat of adsorption, while the optimized lattice model suggests repulsive

adsorbate–adsorbate forces. To explore this difference, it is insightful to understand the uncertainty associated with the extraction of the second virial coefficient from the experimental adsorption data.

Kiselev [61] has presented a methodology for extraction of heats of adsorption and adsorbate–adsorbate intermolecular forces based upon the virial equation approach. The methodology requires fitting an exponential form of the virial equation, known as the Wilkins equation, to experimental adsorption isotherms over a range of temperatures

$$p = a \exp\left(\sum_{i=1}^{n} C_i a^{i-1}\right). \tag{12}$$

Here p is the pressure, a is the loading, and C_i, are constants. In Ref. [61] it is suggested that Eq. (12) is capable of capturing the loading behavior to up to 75% of the saturation loading. Assuming temperature independent heat of adsorption (Q_1) and second virial coefficient (Q_2), the system properties can be linearly related to the constants (C_i) as

$$C_i = B_i - Q_i/\mathrm{RT}.$$

Note that the temperature insensitivity is a potentially poor assumption for the benzene-NaX system where temperature dependent partitioning conceivably occurs between the two types of binding sites.

The propagation of error in first extracting C_i from isotherms over a range of temperatures and then employing them to extract Q_i is evidenced in Fig. 12.

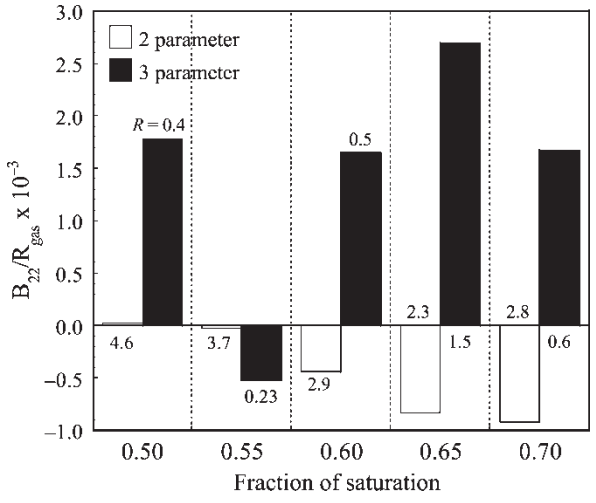

FIGURE 12 Second virial coefficients extracted from the experimental adsorption isotherms by fitting fractions of the isotherms indicated, with two (clear bars) and three parameters (solid bars) showing both attractive ($B_{22} < 0$) and repulsive ($B_{22} > 0$) forces. The residuals, R, are a measure of the fit of the model to the experimental adsorption isotherms over the full range of pressures.

Here we employ two and three constants in the Wilkins expression for extracting the second virial coefficient from different pressure ranges of the experimental adsorption isotherms. In contrast to the relative invariance of the heat of adsorption (not shown), the extracted second virial coefficient varies considerably with the fitting technique and pressure range. As reflected by the approximate order of magnitude difference in the respective residuals, R, a three parameters model fits better than the two-parameter one. However, for comparable residuals, the extracted adsorbate–adsorbate forces can be attractive ($B_{22} < 0$) or repulsive ($B_{22} > 0$) with a wide range of absolute strengths depending on the pressure range of the adsorption isotherm employed in the fitting. This dependence of the adorbate–adsorbate interactions upon the fitting underscores the inherent uncertainty in the base intermolecular forces and motivates the alternative approach to model parameterization discussed in this paper.

References

[1] Demontis, P. and Suffritti, G.P. (1997) "Structure and dynamics of zeolites investigated by molecular dynamics", *Chem. Rev.* **97**, 2845.

[2] Maginn, E.J., Bell, A.T. and Theodorou, D.N. (1993) "Transport diffusivity of methane in silicalite from equilibrium and nonequilibrium simulations"", *J. Phys. Chem.* **97**, 4173.

[3] Theodorou, D.N., Snurr, R.Q. and Bell, A.T. (1996) "Molecular dynamics and diffusion in microporous materials", In: Alberti, G. and Bein, T., eds, *Comprehensive Supramolecular Chemistry* (Pergamon Press, New York), p 507.

[4] Skoulidas, A.I. and Sholl, D.S. (2001) "Direct test of the Darken approximation for molecular diffusion in zeolites using equilibrium molecular dynamics", *J. Phys. Chem. B* **105**, 3151.

[5] Vlugt, T.J.H., Krishna, R. and Smit, B. (1999) "Molecular simulations of adsorption isotherms for linear and branched alkanes and their mixtures in silicalite", *J. Phys. Chem. B* **103**, 1102.

[6] Bell, A.T., Maginn, E.J. and Theodorou, D.N. (1997) "Molecular simulation of adsorption and diffusion in zeolites", In: Ertl, G., Knozinger, H. and Weitkamp, J., eds, *Handbook of Heterogeneous Catalysis* (Wiley-VCH, Weinheim, Germany), p 1165.

[7] Smit, B. and Siepmann, J.I. (1994) "Simulating the adsorption of alkanes in zeolites", *Science* **264**, 1118.

[8] Snurr, R.Q., Bell, A.T. and Theodorou, D.N. (1993) "Prediction of adsorption of aromatic hydrocarbons in silicalite from Grand Canonical Monte Carlo Simulations with biased insertions", *J. Phys. Chem.* **97**, 13742.

[9] van Tassel, P.R., Somers, S.A., Davis, H.T. and McCormick, A.V. (1994) "Lattice model and simulation of dynamics of adsorbate motion in zeolites", *Chem. Eng. Sci.* **49**, 2979.

[10] Nelson, P.H., Kaiser, A.B. and Bibby, D.M. (1991) "Simulation of diffusion and adsorption in zeolites", *J. Catal.* **127**, 101.

[11] Auerbach, S.M. (2000) "Theory and simulation of jump dynamics, diffusion and phase equilibrium in nanopores", *Int. Rev. Phys. Chem.* **19**, 155.

[12] Snurr, R.Q., Bell, A.T. and Theodorou, D.N. (1994) "A hierarchical atomistic lattice simulation approach for the prediction of adsorption thermodynamics of benzene in silicalite", *J. Phys. Chem.* **98**, 5111.

[13] Theodorou, D.N. and Wei, J. (1983) "Diffusion and reaction in blocked and high occupancy zeolite catalysts", *J. Catal.* **83**, 205.
[14] Gladden, L.F., Hargreaves, M. and Alexander, P. (1999) "Monte Carlo lattice dynamics studies of binary adsorption in silicalite", *Chem. Eng. J.* **74**, 57.
[15] Coppens, M.O., Bell, A.T. and Chakraborty, A.K. (1998) "Effect of topology and molecular occupancy on self-diffusion in lattice models of zeolites-Monte Carlo simulations", *Chem. Eng. Sci.* **53**, 2053.
[16] Coppens, M.O., Bell, A.T. and Chakraborty, A.K. (1999) "Dynamic Monte-Carlo and mean-field study of the effect of strong adsorption sites on self-diffusion in zeolites", *Chem. Eng. Sci.* **54**, 3455.
[17] Keil, F.J., Krishna, R. and Coppens, M.O. (2000) "Modeling of diffusion in zeolites", *Rev. Chem. Eng.* **16**, 71.
[18] Raimondeau, S., Aghalayam, P., Mhadeshwar, A.B. and Vlachos, D.G. (2003) "Parameter optimization in molecular models: application to surface kinetics", *Ind. Eng. Chem. Res.* **42**, 1174.
[19] Fitch, A.N., Jobic, H. and Renouprez, A. (1986) "Localization of benzene in sodium-Y zeolite by powder neutron diffraction", *J. Phys. Chem.* **80**, 1311.
[20] Olsen, D.H. (1995) "The crystal structure of dehydrated NaX", *Zeolites* **15**, 439.
[21] Vitale, G., Mellot, C.F., Bull, L.M. and Cheetham, A.K. (1997) "Neutron diffraction and computational study of zeolite NaX: influence of SIII' cations on its complex with benzene", *J. Phys. Chem. B* **101**, 4559.
[22] Barrer, R.M. (1964) "Molecular sieves", *Endeavour* **23**, 122.
[23] Ruthven, D.M. and Doetsch, I.H. (1976) "Diffusion of hydrocarbons in 13X zeolite", *AIChE J.* **22**, 882.
[24] Germanus, A., Karger, J., Pfeifer, H., Samulevic, N.N. and Zdanov, S.P. (1985) "Intracrystalline self-diffusion of benzene, toluene and xylene isomers in zeolites Na-X", *Zeolites* **5**, 91.
[25] Saravanan, C. and Auerbach, S.M. (1999) "Theory and simulation of cohesive diffusion in nanopores: transport in subcritical and supercritical regimes", *J. Chem. Phys.* **110**, 11000.
[26] Dymond, J.H. and Smith, E.B. (1969) *The Virial Coefficients of Gases* (Oxford University Press, New York), p 231.
[27] Saravanan, C. and Auerbach, S.M. (1997) "Modeling the concentration dependence of diffusion in zeolites. I. Analytical theory for benzene in Na-Y", *J. Chem. Phys.* **107**, 8120.
[28] Saravanan, C. and Auerbach, S.M. (1997) "Modeling the concentration dependence of diffusion in zeolites. II. Kinetic Monte Carlo simulations of benzene in Na-Y", *J. Chem. Phys.* **107**, 8132.
[29] Saravanan, C., Jousse, F. and Auerbach, S.M. (1998) "Modeling the concentration dependence of diffusion in zeolites. III. Testing mean field theory for benzene in Na-Y with simulation", *J. Chem. Phys.* **108**, 2162.
[30] Reese, J.S., Raimondeau, S. and Vlachos, D.G. (2001) "Monte Carlo algorithms for complex surface reaction mechanisms: efficiency and accuracy", *J. Comput. Phys.* **173**, 302.
[31] Saravanan, C., Jousse, F. and Auerbach, S.M. (1998) "Ising model of diffusion in molecular sieves", *Phys. Rev. Lett.* **80**, 5754.
[32] Hood, S., Toby, B.H. and Weinberg, W.H. (1985) "Precursor--mediated molecular chemisorption and thermal desorption—the interrelationships among energetics, kinetics, and adsorbate lattice structure", *Phys. Rev. Lett.* **55**, 2437.
[33] Auerbach, S.M. and Metiu, H.I. (1996) "Diffusion in zeolites via cage-to-cage kinetics: Modeling benzene diffusion in Na-Y", *J. Chem. Phys.* **105**, 3753.
[34] Auerbach, S.M., Henson, N.J., Cheetham, A.K. and Metiu, H. (1995) "Transport theory for cationic zeolites: Diffusion of benzene in Na-Y", *J. Phys. Chem.* **99**, 10600.
[35] Ford, D.M. and Glandt, E.D. (1995) "Steric hindrance at the entrances to small pores", *J. Membr. Sci.* **107**, 47.
[36] Ford, D.M. and Glandt, E.D. (1995) "Molecular simulation study of the surface barrier effect. Dilute gas limit", *J. Phys. Chem.* **99**, 11543.
[37] Mhadeshwar, A.B., Wang, H. and Vlachos, D.G. (2003) "Thermodynamic consistency in microkinetic development of surface reaction mechanisms", *J. Phys. Chem. B* **107**, 12721.
[38] Barthomeuf, D. and Ha, B.H. (1973) "Adsorption of benzene and cyclohexane on Faujasite-type zeolites. Part 1: thermodynamic properties at low coverage", *J. Chem. Soc. Faraday Trans.* **69**, 2147.
[39] Barthomeuf, D. and Ha, B.H. (1973) "Adsorption of benzene and cyclohexane on Faujasite-type zeolites. Part 2: adsorption site efficiency and zeolite field influence at high coverage", *J. Chem. Soc. Faraday Trans.* **69**, 2158.
[40] Mosell, T., Schrimpf, G. and Brickmann, J. (1997) "Diffusion of aromatic molecules in zeolite NaY. 2. Dynamical corrections", *J. Phys. Chem. B* **101**, 9485.
[41] Mosell, T., Schrimpf, G. and Brickmann, J. (1997) "Diffusion of aromatic molecules in zeolite NaY. 1. Constrained reaction coordinate dynamics", *J. Phys. Chem. B* **101**, 9476.
[42] Jousse, F. and Auerbach, S.M. (1997) "Activated diffusion of benzene in Na-Y: rate constants from transition state theory with dynamical corrections", *J. Chem. Phys.* **107**, 9629.
[43] Katsoulakis, M., Majda, A.J. and Vlachos, D.G. (2003) "Coarse-grained stochastic processes for microscopic lattice systems", *Proc. Natl Acad. Sci.* **100**, 782.
[44] Katsoulakis, M.A., Majda, A.J. and Vlachos, D.G. (2003) "Coarse-grained stochastic processes and Monte Carlo simulations in lattice systems", *J. Comput. Phys.* **186**, 250.
[45] Katsoulakis, M.A. and Vlachos, D.G. (2000) "From microscopic interactions to macroscopic laws of cluster evolution", *Phys. Rev. Lett.* **84**, 1511.
[46] Lam, R., Basak, T., Vlachos, D.G. and Katsoulakis, M.A. (2001) "Validation of mesoscopic theories and their application to computing effective diffusivities", *J. Chem. Phys.* **115**, 11278.
[47] Snyder, M.A., Vlachos, D.G. and Katsoulakis, M.A. (2003) "Mesoscopic modeling of transport and reaction in microporous crystalline membranes", *Chem. Eng. Sci.* **58**, 895.
[48] Vlachos, D.G. and Katsoulakis, M.A. (2000) "Derivation and validation of mesoscopic theories for diffusion of interacting molecules", *Phys. Rev. Lett.* **85**, 3898.
[49] Petzold, L.R. (1983) "Automatic selection of methods for solving stiff and nonstiff systems of ordinary differential equations", *SIAM J. Sci. Stat. Comput.* **4**, 136.
[50] Hindmarsh, A.C. (1983) "ODEPACK, a systematized collection of ODE solvers", In: Stepleman, R.S., *et al.*, eds, *Scientific Computing* (North-Holland Publishing Co., Amsterdam), p 55.
[51] Box, G.E.P. and Draper, N.R. (1987) *Empirical Model-building and Response Surfaces* (Wiley, New York).
[52] Davis, S.G., Mhadeshwar, A.B., Vlachos, D.G. and Wang, H. (2003) "A new approach to response surface development for detailed gas-phase and surface reaction kinetic model development and optimization", *Int. J. Chem. Kinetics*, in press.
[53] Ruthven, D.M. and Goddard, M. (1984) "Correlation and analysis of equilibrium isotherms for hydrocarbons on zeolites", In: Myers, A.L. and Belfort, G., eds, Fundamentals of adsorption: Proceedings of the Engineering Foundation Conference held at Schloss Elmau, Bavaria, West Germany, May 6–11, 1983 (Engineering Foundation, New York), p 533.
[54] Ciraolo, M.F., Hanson, J.C., Norby, P. and Grey, C.P. (2001) "Combined X-ray and neutron powder refinement and NMR study of hydrochlorofluorocarbon HCFC-124a (CF2HCF2Cl) binding on NaX", *J. Phys. Chem. B* **105**, 12330.
[55] Lim, K.H. and Grey, C.P. (2000) "Characterization of extra-framework cation positions in zeolites NaX and NaY with very fast Na-23 MAS and multiple quantum MAS NMR spectroscopy", *J. Am. Chem. Soc.* **122**, 9768.
[56] Grey, C.P., Poshni, F.I., Gualtieri, A.F., Norby, P., Hanson, J.C. and Corbin, D.R. (1997) "Combined MAS NMR and X-ray powder diffraction structural characterization of hydrofluorocarbon-134 adsorbed on zeolite NaY: observation of cation migration and strong sorbate–cation interactions", *J. Am. Chem. Soc.* **119**, 1981.
[57] Jobic, H., Bee, M. and Pouget, S. (2000) "Diffusion of benzene in ZSM-5 measured by the neutron spin-echo technique", *J. Phys. Chem. B* **104**, 7130.
[58] Clark, L.A. and Snurr, R.Q. (1999) "Adsorption isotherm sensitivity to small changes in zeolite structure", *Chem. Phys. Lett.* **308**, 155.

[59] Jaramillo, E., Grey, C.P. and Auerbach, S.M. (2001) "Molecular dynamics studies of hydrofluorocarbons in faujasite-type zeolites: modeling guest-induced cation migration in dry zeolites", *J. Phys. Chem. B* **105**, 12319.
[60] Papaioannou, C., Petroutsos, G. and Gunsser, W. (1997) "Examination of the adsorption of hydrocarbons at low coverage on faujasite zeolites", *Solid State Ionics* **799**, 101–103.
[61] Kiselev, A.V. (1971) "Vapor adsorption on zeolites considered as crystalline specific adsorbents", *Adv. Chem.* **102**, 37.
[62] Bezus, A.G., Kiselev, A.V., Sedlacek, Z. and Du, P.Q. (1971) "Adsorption of ethane and ethylene on X-zeolites containing Li+, Na+, K+, Rb+ and Cs+ cations", *Trans. Faraday Soc.* **67**, 468.